ARMY RESEARCH LABORATORY

The Low-Temperature Vibrational Behavior of Pentaerythritol Tetranitrate

by Jennifer A. Ciezak and Timothy A. Jenkins

ARL-TR-4470 June 2008

NOTICES

Disclaimers

The findings in this report are not to be construed as an official Department of the Army position unless so designated by other authorized documents.

Citation of manufacturer's or trade names does not constitute an official endorsement or approval of the use thereof.

Destroy this report when it is no longer needed. Do not return it to the originator.

Army Research Laboratory
Aberdeen Proving Ground, MD 21005-5066

ARL-TR-4470 **June 2008**

The Low-Temperature Vibrational Behavior of Pentaerythritol Tetranitrate

Jennifer A. Ciezak
Weapons and Materials Research Directorate, ARL

Timothy A. Jenkins
Carnegie Institution of Washington

REPORT DOCUMENTATION PAGE	Form Approved OMB No. 0704-0188

1. REPORT DATE *(DD-MM-YYYY)*	2. REPORT TYPE	3. DATES COVERED (From - To)
June 2008	Final	January 2007–October 2007

4. TITLE AND SUBTITLE
The Low-Temperature Vibrational Behavior of Pentaerythritol Tetranitrate

5a. CONTRACT NUMBER

5b. GRANT NUMBER

5c. PROGRAM ELEMENT NUMBER

6. AUTHOR(S)
Jennifer A. Ciezak and Timothy A. Jenkins*

5d. PROJECT NUMBER
IHEM01A

5e. TASK NUMBER

5f. WORK UNIT NUMBER

7. PERFORMING ORGANIZATION NAME(S) AND ADDRESS(ES)
U.S. Army Research Laboratory
ATTN: AMSRD-ARL-WM-BD
Aberdeen Proving Ground, MD 21005-5066

8. PERFORMING ORGANIZATION REPORT NUMBER
ARL-TR-4470

9. SPONSORING/MONITORING AGENCY NAME(S) AND ADDRESS(ES)

10. SPONSOR/MONITOR'S ACRONYM(S)

11. SPONSOR/MONITOR'S REPORT NUMBER(S)

12. DISTRIBUTION/AVAILABILITY STATEMENT
Approved for public release; distribution is unlimited.

13. SUPPLEMENTARY NOTES
*Geophysical Laboratory, Carnegie Institution of Washington, 5251 Broad Branch Rd. NW, Washington, DC 20015

14. ABSTRACT
The authors report the room temperature Raman and synchrotron Fourier transform infrared measurements of pentaerythritol tetranitrate (PETN), as well as low-temperature Raman measurements from 4 to 298 K up to ~15 GPa, using a helium gas-pressure medium. No evidence of phase transitions was observed in the pressure/temperature range studied, although the molecular symmetry of PETN is modified from S4 to D2 near 8.1 GPa. The modification was not found to be temperature dependent, and decompression studies indicated the reversibility of the symmetry change.

15. SUBJECT TERMS
vibrational spectroscopy, high pressure, pentaerythritol tetranitrate, diamond anvil cell, PETN

16. SECURITY CLASSIFICATION OF:			17. LIMITATION OF ABSTRACT	18. NUMBER OF PAGES	19a. NAME OF RESPONSIBLE PERSON
a. REPORT	b. ABSTRACT	c. THIS PAGE			Jennifer A. Ciezak
UNCLASSIFIED	UNCLASSIFIED	UNCLASSIFIED	UL	24	19b. TELEPHONE NUMBER (*Include area code*) 410-306-1904

Standard Form 298 (Rev. 8/98)
Prescribed by ANSI Std. Z39.18

Contents

List of Figures

List of Tables

Acknowledgments

Dr. K. Clark of the Naval Surface Warfare Center, Indian Head, MD, is thanked for providing the pentaerythritol tetranitrate crystals. We also thank Dr. R. J. Hemley for valuable suggestions during the preparation of this report.

1. Introduction

The energetic material pentaerythritol tetranitrate (PETN), shown in figure 1, is extensively used in military applications as an initiating or boosting high explosive. Nearly two decades ago, PETN was subjected to numerous characterization studies aimed at understanding a wide variety of its chemical and physical properties that relate to its sensitivity, stability, and performance (*1*). The stability of the material under high temperature has been investigated, and several mechanisms of decomposition are known (*2*). Several experiments were also performed under high pressure to discern the behavior of PETN under high density (*3–6*), and a phase transition was reported near 4.3 GPa using neutron diffraction (*7*). Due to the experimental limitations that existed at the time, only pressures below 10 GPa were obtainable. However, with the advent of readily available diamond anvil cells, there has been a rising interest in the past 5 years in the high-pressure behavior of energetic materials.

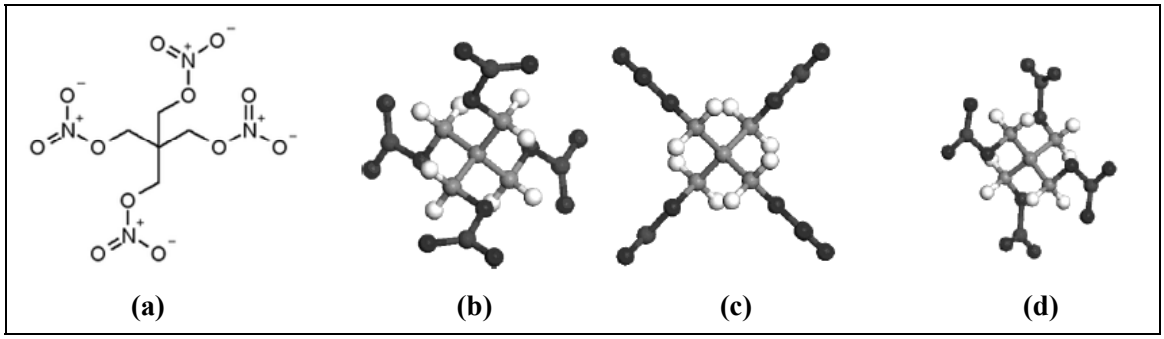

Figure 1. The energetic material PETN: (a) the molecular schematic ($C(CH_2ONO_2)_4$), (b) the S_4 molecular symmetry, (c) the D_2 molecular symmetry, and (d) the $C_2(\alpha)$ molecular symmetry.

At atmospheric pressure, below the melting temperature of 141.3 °C (*1*), PETN appears as white crystals assembled into a tetragonal structure ($P\text{-}42_1c$) with four molecules per unit cell arranged in an S_4 molecular symmetry. Both infrared (*6*, *8*, *9*) and Raman (*9–10*) characterizations of this phase exist, and several theoretical calculations of the vibrational frequencies of the crystal have been reported (*8–13*). The mechanical properties of PETN at ambient conditions are quite interesting, as PETN exhibits a strong directional dependence to shock-initiated detonation (*5*, *14–22*). Although PETN is classified as quite easily detonated by shock, several directions of impact with respect to the crystal structure exist that will not cause detonation, even when the shock wave fully crosses the crystal. Researchers have found that shock-initiated detonation occurs along the a-axis of the crystal but not along the c-axis (*14–22*).

The behavior of PETN under high-pressure conditions is quite controversial. A high-pressure phase transition was reported during a Raman spectroscopic study near 5 GPa (*23*), which corroborated with the earlier neutron diffraction study (*7*). A detailed comparison of the experimental vibrational frequencies obtained under high-pressure conditions to calculated vibrational frequencies of various conformers of PETN with different molecular symmetry provided evidence for a molecular symmetry change (S_4 to C_2) (*23*). Subsequent experimental studies have reported modifications in the Raman spectra and x-ray diffraction patterns, such as the appearance or disappearance of peaks, large spectroscopic shifts of the Raman frequencies to higher energies, and splitting of the x-ray diffraction peaks (*12*, *24–26*). Recently, changes in the vibrational patterns were shown to be strongly dependent upon the stress and strain within the sample. Stress within the diamond anvil cell can be controlled through the use of different pressure-transmitting media, which decreases or increases the strain within the sample. Under hydrostatic conditions with nearly no sample strain, the modifications in the vibrational spectra indicated a symmetry change to the D_2 molecular geometry, but no crystallographic phase transition was observed between ambient pressure and 14 GPa. Several less hydrostatic samples with a higher degree of stress/strain showed a significant loss of vibrational resolution in both the number of visible peaks and intensity, presumably due to the activation of the PETN slip planes (*27*). The loss of intensity, coupled with the disappearance of several vibrational peaks, may have been misconstrued as a phase transition (*27*).

In the past year, a combined experimental/theoretical report (*28*) provided new evidence for Dreger's earlier proposal (*23*) that PETN undergoes a structural transition below 6 GPa to an orthorhombic phase with a space group of $P2_12_12$. The quantum chemical calculations employed in this study indicated a shear-stress-induced transition, which is ferroelastic in nature. Such a phase transition allows for the possibility of soft shear components to propagate along specific directions within the PETN molecule, which may relate to the observed dependence of the shock sensitivity to crystalline orientation (*28*). However, this suggestion was based on Landau theory which is not entirely valid at high pressures since many variables of the theory assume any change in volume is negligible (*29*). Upon pressure increase, Landau theory dictates the values of all parameters will change due to the volume variation with pressure, which limits its applicability at variable pressures.

Although PETN is well characterized under a wide variety of extreme conditions, such as high temperature and high pressure, the behavior of PETN is still largely unknown within certain temperature and pressure ranges. To expand the available knowledge of PETN, Raman spectroscopic investigations were undertaken as a function of both temperature and pressure within the ranges of 20 to 298 K and ambient pressure to 14 GPa. Additionally, if PETN undergoes a ferroelectric phase transition near 5 GPa, evidence of the transition is expected to become increasingly apparent at low temperatures. This is due to a decrease in thermal motion which tends to destroy the ferroelectric disorder at higher temperatures. The results presented

here expand, in depth, upon previously reported material and are part of a research program aimed at extending the current understanding of pressure-driven structural transitions of energetic materials through employment of a multitechnique approach.

2. Experimental Methodology

Large grains of polycrystalline PETN were obtained from the Naval Surface Warfare Center at Indian Head, MD, and used without further purification. Single crystals of PETN with an approximate diameter of 175 μm and a thickness between 35 and 60 μm were selected from the polycrystalline sample and loaded into the center of a rhenium gasket hole with a diameter of 250 μm. Helium gas, which was used as the pressure-transmitting medium for all experimental measurements, was loaded into the Mao–Bell diamond anvil cell (DAC) using a specialized gas chamber discussed elsewhere (*30*). The DAC was mounted in a cryostat equipped with a spring-loaded lever arm system, which enables the user to both increase and decrease the pressure from outside the cryostat. The temperature was monitored and controlled through two resistive heaters and a diode sensor attached to the DAC.

In situ Raman spectra of PETN were measured to pressures near 15 GPa and temperatures between 20 K and 298 K. The pressure on the sample was determined from the frequency shift of the R_1 fluorescence line (*31*). The excitation radiation was an argon ion laser (Coherent Innova 90) operating at 488 nm with a power of 0.5 W with a laser spot size of ~7 μm in diameter. A 460-mm focal length f/5.3 imaging spectrograph (ISA HR 460) equipped with an 1800-groves/mm grating, which provides a spectral resolution of ±4.0 cm^{-1}, was used for all Raman experiments. Prior to any experimental measurements, a wavelength calibration of the spectrograph was performed with a neon lamp; this method of calibration has an accuracy of ±1.0 cm^{-1} (*32*).

Synchrotron infrared (IR)-absorption experiments were performed at beamline U2A of the National Synchrotron Light Source of Brookhaven National Laboratory. The synchrotron light is extracted from the vacuum ultraviolet storage ring in a 40- × 40-mrad solid angle. The collimated beam is delivered through a vacuum pipe system and directed into a Bruker IFS 66v Fourier transform infrared spectrometer. Extensive detail of the optical layout of this beamline is available (*33*). The resolution used for all measurements was 4 cm^{-1}.

3. Results and Discussion

When compressed at room temperature (298 K), PETN shows a change in the molecular symmetry from $S_4 \rightarrow D_2$ between 6.3 and 10.9 GPa (figures 2 and 3). The exact pressure of the symmetry transformation is known to be strongly dependent on the conditions within the cell as well as the crystalline phase (i.e., powder or single crystal) (*27*), but in this work, the transition pressure was near 8.1 GPa. The transformation can be visually observed since single-crystal PETN normally appears translucent, but after the transformation, the sample looks slightly opaque. In most cases, the transformation happens instantaneously and goes to completion within seconds as determined by Raman spectroscopy. This transformation can be detected by the splitting of several vibrational modes in the Raman spectrum (figure 2) and by the fluctuations in the infrared intensity over the pressure range studied (figure 3). The value of the pressure onset of the modification in the molecular symmetry is not temperature dependent within the range of 20 to 298 K (figures 2–6), suggesting the geometry modification observed near 8.1 GPa is not ferroelastic in nature. Data taken upon pressure release and compared to the data from the compression sequence did not reveal any measurable differences in the frequencies, although the vibrational intensities were much lower in the recovered sample. This can be attributed to the crystalline damage that occurs as the slip planes are activated (*27*, *34*).

Figures 4–6 show the temperature-dependent Raman spectra of single-crystal PETN as a function of pressure. The low-temperature Raman spectra of PETN are very similar to those obtained at higher temperatures, although at lower temperatures considerably more peaks are observed. The increased number of peaks at low temperatures partially results from increased vibrational splitting as a larger percentage of molecules occupy the ground state, as well as an inherent design problem with the cryostat, which permits small vibrational oscillations as the spectra are being collected. A broad fluorescence background appears in several spectra that may indicate sample damage. Also, at the present time it remains very difficult to collect the IR spectra at low temperature due to the optical setup at the synchrotron. As a result, all IR measurements were performed at room temperature.

The pressure dependences of the wavenumbers of the vibrational bands differ slightly among the different temperatures measured, but there is no abrupt shift near 8.1 GPa as the geometry transformation occurs. The frequency shifts ($\delta\nu/\delta P$) of the vibrational bands at different temperatures are summarized in table 1. Interestingly, the majority of the vibrational bands show mode hardening upon decreasing temperature as indicated by an increase in $\delta\nu/\delta P$. Mode hardening clearly indicates that the local ordering of the molecule changes with decreasing temperature, but this phenomenon may closely correlate with the pronounced brittleness of PETN at a low temperature. In contrast to other energetic materials, the brittleness of PETN becomes increasingly evident under conditions of large stress/strain due to the strong anisotropic behavior along particular crystalline slip planes. As the material contracts at low temperatures, small crystalline voids may occur which readily propagate along the slip planes.

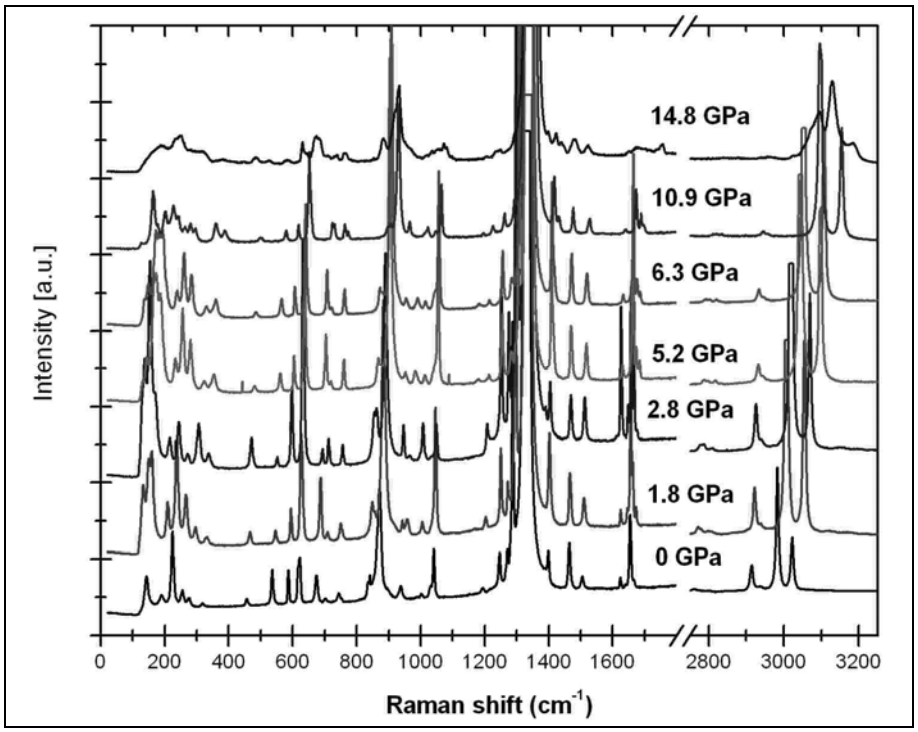

Figure 2. Representative Raman spectra of a single-crystal PETN compressed with a helium pressure medium at 298 K. The strong first order scattering from the diamond anvils is observed in the spectral range between 1300 and 1400 cm^{-1}. The intensity of this feature is truncated for better resolution of the PETN vibrational peaks. The spectral region between 1700 and 2700 cm^{-1} is omitted because of the low vibrational intensity observed. Each Raman profile is vertically scaled for the sake of clarity.

In these experiments, the largest degree of mode hardening is observed for the CH_2 stretches with average changes of (1.5 cm^{-1}/GPa)/K. This seems to be quantitatively correct as a primary shear plane lies perpendicular to the CH_2 groups.

Surprisingly, the S_4 and D_2 molecular geometries have a very large domain of pressure and temperature metastability. The pressure dependence of the Raman and IR spectra were studied in wide pressure range at 300 K and at low temperatures. It is somewhat surprising that the D_2 molecular symmetry remains energetically favorable at low temperatures and high pressures, as it is not the most compact. On average, the lower symmetry conformers, such as C_2 (α) (figure 1), of PETN take up ~10% less space than the D_2 conformer. At higher compressions, the increase in the van der Waals repulsions becomes comparable with the intramolecular repulsion forces that control the molecular geometry. Because other conformers are more compact than the D_2 conformer, they will produce less intermolecular repulsion energy in the crystal. It is expected that when the energy gain exceeds the energy gap between the conformers, the PETN molecules will be forced to change conformation. However, there is no evidence of an additional symmetry change at higher pressures, so another factor must play a role in the stabilization of the D_2 conformer. It is suspect that the presence of the shear planes stabilizes the D_2 conformer at such extreme conditions, and further experiments are being pursued to confirm this.

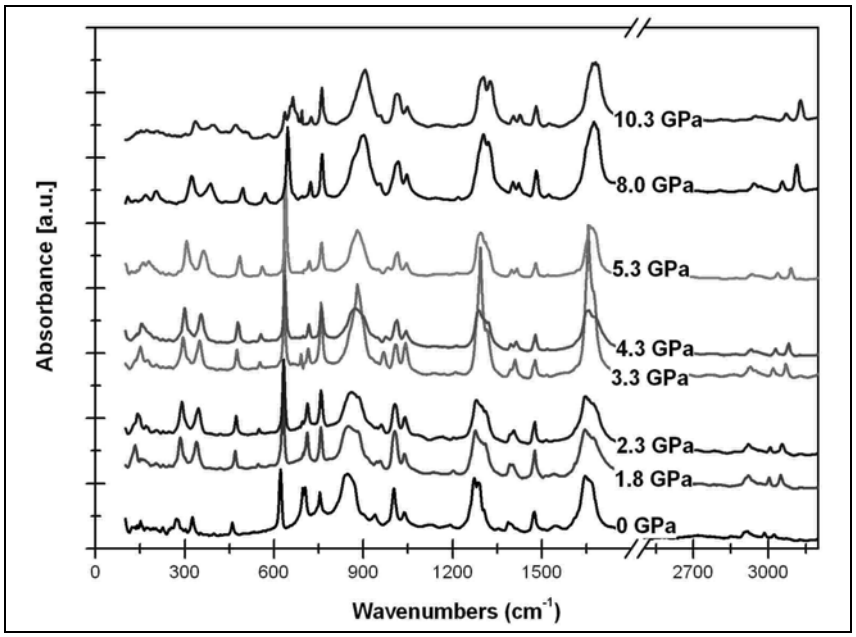

Figure 3. Representative IR spectra of powdered PETN compressed with a helium-pressure medium at 298 K. The spectral region between 1800 and 2600 cm^{-1} is omitted because of the strong nitrogen absorption of the diamond anvils within this spectral range. Each vibrational profile is vertically scaled for the sake of clarity.

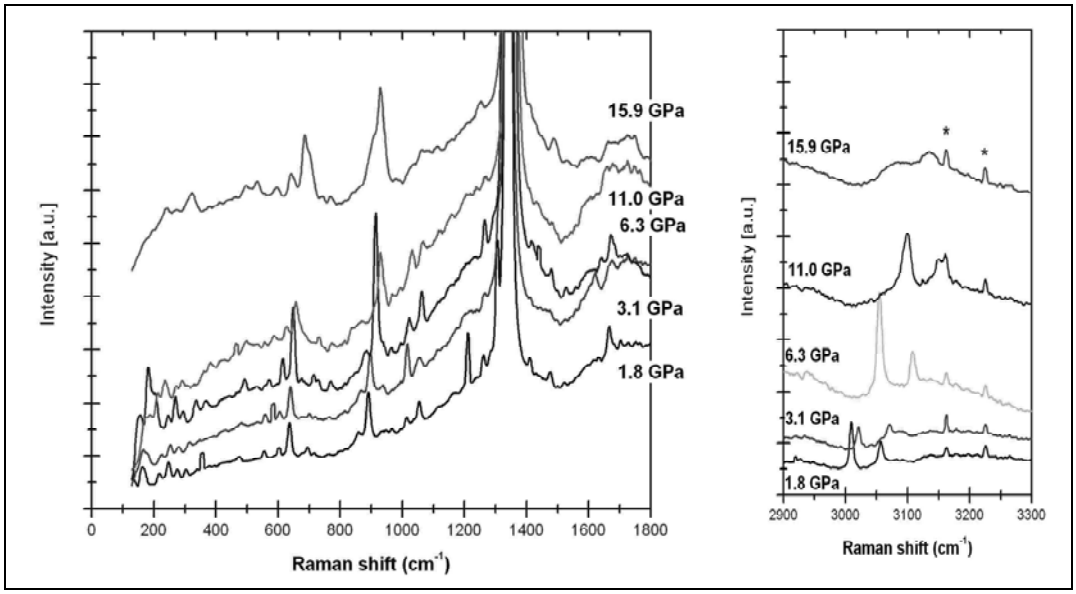

Figure 4. Representative Raman spectra of single-crystal PETN compressed with a helium-pressure medium at 225 K within the spectral range of 150 to 1800 cm^{-1} (left) and 2900 to 3300 cm^{-1} (right). Strong first order scattering from the diamond anvils appears in the spectra between 1300 and 1400 cm^{-1}. The intensity of this feature is truncated for better resolution of the PETN vibrational peaks. Each Raman profile is vertically scaled for the sake of clarity. Asterisks near 3150 and 3275 cm^{-1} indicate vibrational features that do not arise from PETN.

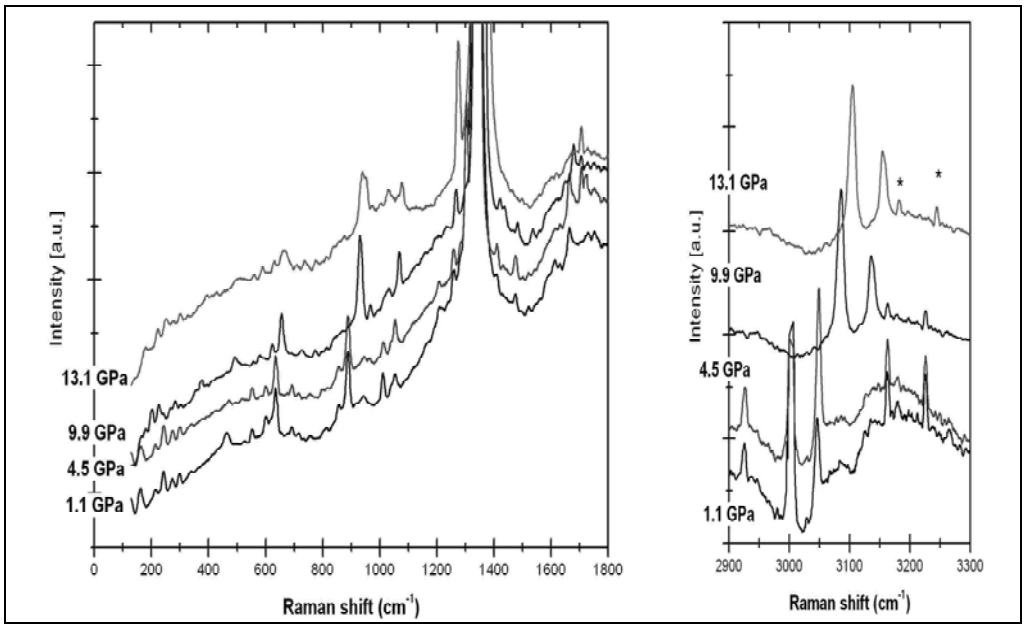

Figure 5. Representative Raman spectra of single-crystal PETN compressed with a helium-pressure medium at 100 K within the spectral range of 150 to 1800 cm^{-1} (left) and 2900 to 3300 cm^{-1} (right). Strong first order scattering from the diamond anvils appears in the spectra between 1300 and 1400 cm^{-1}. The maxima is truncated to permit better resolution of the PETN vibrational peaks. Each Raman profile is vertically scaled for the sake of clarity. Asterisks near 3150, 3275, and 3240 cm^{-1} indicate vibrational features that do not arise from PETN.

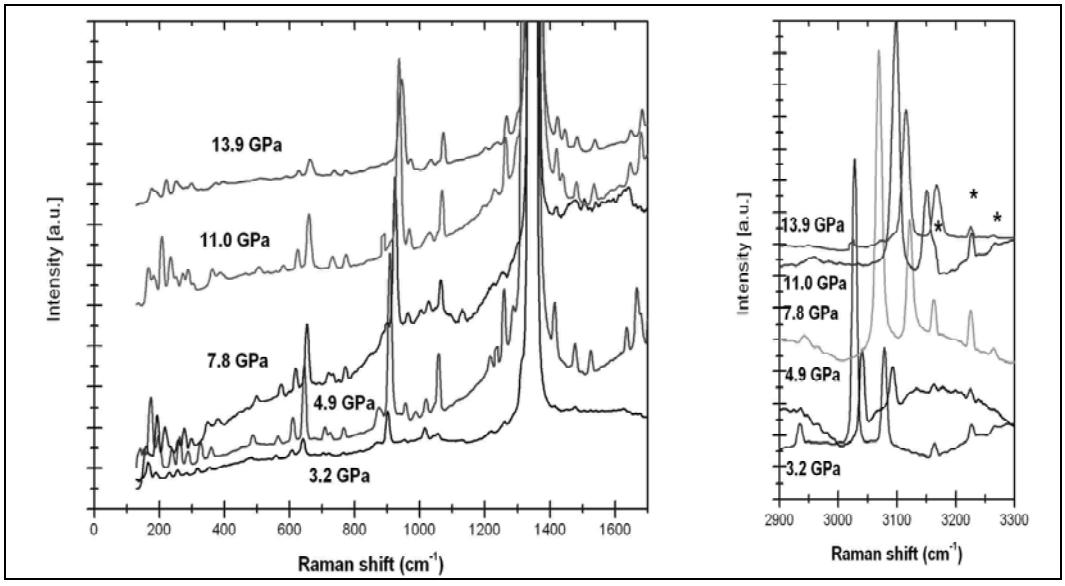

Figure 6. Representative Raman spectra of single-crystal PETN compressed with a helium-pressure medium at 20 K within the spectral range of 150 to 1700 cm^{-1} (left) and 2900 to 3300 cm^{-1} (right). Strong first order scattering from the diamond anvils appears in the spectra between 1300 and 1400 cm^{-1}. The intensity of this feature is truncated for better resolution of the PETN vibrational peaks. Each Raman profile is vertically scaled for the sake of clarity. Asterisks near 3150 and 3275 cm^{-1} indicate vibrational features that do not arise from PETN.

Table 1. Summary of available spectroscopic data for PETN. Raman and IR measurements are reported from this study at room temperature, as well as previously reported IR (*9*), Raman (*9*), and neutron (*13*) vibrational data. Mode shifts (δν [cm^{-1}]/δP [GPa]) are the second-order polynomial slopes of the frequencies with respect to pressure and are shown for various temperatures.

Raman					IR		Previously Reported Experimental Values				
cm^{-1} (298 K)	**δν /δP (298 K)**	**δν/δP (225 K)**	**δν/δP (100 K)**	**δν/δP (20 K)**	**cm^{-1} (298 K)**	**δν/δP (298 K)**	**IR[b] (cm^{-1})**	**Raman[b] (cm^{-1})**	**Neutron[c] (cm^{-1})**	**Assignment[a]**	**Mode No.[a]**
—	—	—	—	3.36	—	—	—	—	127	CC t	9
144	5.20	—	—	3.14	150	5.30	—	—	151	C-O-N w	10
189	3.91	—	—	4.67	—	—	—	—	194	O-CH_2t + CCC def	12
—	—	3.70	3.43	—	—	—	—	—	210	$CONO_2$ r	13
225	3.21	—	—	3.72	228	–0.10	—	—	226	Combination bands	—
255	3.66	4.84	2.75	3.50	—	—	—	—	250	ONO_2 + C_5 skel	14
278	4.10	3.90	3.30	3.43	272	6.18	—	—	274	Combination band	—
324	4.64	4.59	4.50	4.45	326	6.71	—	319	315	CH_2 r + CCC def	17
—	—	3.73	—	3.43	—	—	—	—	347	Combination band	—
—	—	—	—	—	396	7.42	—	—	403	Combination band	—
—	—	1.26	—	—	—	—	—	—	—	—	—
457	3.74	3.71	4.05	4.01	459	4.27	460	459	484	CCC def + O'N st + NO_2 r	18
534	3.44	—	—	—	—	—	—	539	540	C_5 skel +CH_2 w + O'-N st	19
577	3.93	—	—	—	—	—	—	589	597	CC b + ONO_2 r	20
—	—	2.45	2.85	2.82			619, 618	619	613	C_5 skel + ONO_2r	21
—	—	3.07	3.10	3.25	621	4.12	623, 624	624	—	CCC def + ONO_2r	22
675	3.13	3.21	3.54	3.63	698	–0.29	—	676	669	O'-N st + CC st +NO_2 sc	23
704	3.25	3.30	3.30	3.60	704	2.44	703, 704	704	700	O'-N st + CCC def + NO_2r	24
747	1.69	2.72	2.75	2.77	754	0.56	746, 746	746	740	CCC def + O'-N st	25
—	—	—	–0.31	—	—	—	—	—	751	ONO_2 umb	26
—	—	—	0.23	—	—	—	754, 755	755	766	ONO_2 umb +CCC def	28
842	2.98	2.96	2.97	—	847	1.79	—	—	840	Combination band	—
869	3.17	—	—	2.98	—	—	—	839	842	CC st	29
—	—	3.17	3.35	3.43	900	5.63	—	873	867	O'-N st + CC st	32
939	4.45	4.44	4.89	4.82	941	3.79	—	900	903	CCC def + CH_2 r	33
1006	1.70	1.71	1.84	1.86	1003	0.94	1003, 1003	1004	1005	CO st + CCC def	36
1044	1.76	1.88	1.92	1.95	1036	1.46	—	1044	1048	CH_2 t + CCb	37

Table 1. Summary of available spectroscopic data for PETN. Raman and IR measurements are reported from this study at room temperature, as well as previously reported IR (*9*), Raman (*9*) and neutron (*13*) vibrational data. Mode shifts ($\delta\nu$ [cm^{-1}]/δP [GPa]) are the second-order polynomial slopes of the frequencies with respect to pressure and are shown for various temperatures (continued).

Raman					IR		Previously Reported Experimental Values				
cm^{-1} (298 K)	**$\delta\nu/\delta P$ (298 K)**	**$\delta\nu/\delta P$ (225 K)**	**$\delta\nu/\delta P$ (100 K)**	**$\delta\nu/\delta P$ (20 K)**	**cm^{-1} (298 K)**	**$\delta\nu/\delta P$ (298 K)**	**IR[b] (cm^{-1})**	**Raman[b] (cm^{-1})**	**Neutron[c] (cm^{-1})**	**Assignment[a]**	**Mode No.[a]**
1195	1.98	2.01	2.22	2.30	—	—	1159	—	1160	CH_2 w + C_5 skel	39
1251	1.58	1.57	1.58	1.62	1273	3.00	—	1253	—	CHb	41
—	—	—	1.75	1.82	1305	2.04	1284, 1285	1286	—	NO_2 st + CH b + C_5 skel	44
1402	2.24	2.33	2.37	2.38	1397	2.92	1396, 1396	1397	—	CH_2 w + CCC def	48
1464	1.67	1.59	1.73	1.81	1475	0.56	—	—	—	CH_2 sc	50
1506	2.23	—	2.21	2.25	—	—	1509	1512	—	CH2 sc	51
—	—	—	—	—	1545	2.20	—	1539	—	—	—
1623	2.24	2.28	2.20	2.24	1612	0.90	—	1633	—	NO_2 st (a)	53
1658	1.39	1.26	1.53	—	1647	3.18	1655, 1661	1665	—	NO_2 st (a)	54
2767	4.20	—	3.67	—	2849	0.00	—	—	—	CH_2 st (s)	56
2904	3.30	—	—	—	2904	4.56	—	—	—	CH_2 st (s)	57
2915	5.80	—	—	—	2916	6.13	2910, 2916	2918	—	CH_2 st (a)	61
2971	4.69	—	—	—	2985	8.54	2984, 2985	2987	—	CH_2 st (s)	58
2971	7.06	6.92	8.02	8.50	—	—	—	—	—	CH_2 st (a)	59
3016	7.60	5.60	8.47	9.08	3022	10.48	3023, 3023	3025	—	CH_2 st (a)	60

[a]st = stretch, b = bend, sc = scissors, umb = umbrella, skel = skeletal, t = torsion, def = deformation, r = rock, w = wag, (a) = antisymmetric, (s) = symmetric, and O' = ester oxygen.

[b]Assignments are given based on Gruzdkov and Gupta (*9*).

[c]Unpublished results (*13*).

4. Conclusions

The results discussed herein provide important insights into the behavior of single crystal PETN at high pressure and low temperatures. Instead of a high-pressure phase transition, we find a molecular geometry modification from S_4 to D_2 symmetry. Our data show that the symmetry modification is not temperature dependent and indicates the D_2 geometry is metastable in much of the P-T range over which it is observed, since it is typically obtained only as a result of compression. An important general conclusion of this work is that the high-pressure behavior is more complex than previously thought due to the presence of multiple factors, such as stress/strain and crystal condition, which play a key role in the behavior of the material.

5. References

1. Cady, H. H. *The PETN-DiPEHN-TriPEON System*; LA-4486-MS; Los Alamos National Laboratory: Los Alamos, NM, December 1972.

2. Chambers, D. M. *Perspectives on Pentaerythritol Tetranitrate (PETN) Decomposition*; UCRL-JC-148956; Lawrence Livermore National Laboratory: Livermore, CA, July 2002.

3. Olinger, B.; Halleck, P. M.; Cady, H. H. The Isothermal Linear and Volume Compression of Pentaerythritol Tetranitrate (PETN) to 10 GPa (100 kbar) and the Calculated Shock Compression. *J. Chem. Phys.* **1975**, *62*, 4480.

4. Dick, J. J.; Mulford, R. N.; Spencer, W. J.; Pettit, D. R.; Garcia, E.; Shaw, D. C. Shock Response of Pentaerythritol Tetranitrate Single Crystals. *J. Appl. Phys.* **1991**, *70*, 3572.

5. Halleck, P. M.; Wackerle, J. Dynamic Elastic-Plastic Properties of Single Crystal Pentaerythritol Tetranitrate. *J. Appl. Phys*. **1976**, *47*, 976.

6. Foltz, M. F. Pressure Dependence of the Reaction Propagation Rate of PETN at High Pressure. *Proceedings of the 10th International Detonation Symposium*, Boston, MA, 12–16 July 1993; Office of Naval Research: Arlington, VA, 1993; p 579.

7. Dick, J. J.; von Dreele, R. B. Determination of the Response of Pentaerythritol Tetranitrate to Static High Pressure up to 4.28 GPa by Neutron Diffraction. *AIP Conf. Proc.* **1998**, *429*, 827.

8. Allis, D. G.; Korter, T. M. Theoretical Analysis of the Terahertz Spectrum of the High Explosive PETN. *ChemPhysChem* **2006**, *7*, 2398.

9. Gruzdkov, Y. A.; Gupta, Y. M. Vibrational Properties and Structure of Pentaerythritol Tetranitrate. *J. Phys. Chem. A* **2001**, *105*, 6197.

10. Gruzdkov, Y. A.; Gupta, Y. M. Shock Wave Initiation of Pentaerythritol Tetranitrate Single Crystals: Mechanism of Anisotropic Sensitivity. *J. Phys. Chem. A* **2000**, *104*, 11,169.

11. Sorescu, D. C.; Rice, B. M. Thompson, D. L. Theoretical Studies of the Hydrostatic Compression of RDX, HMX, HNIW, and PETN Crystals. *J. Phys. Chem. B* **1999**, *103*, 6783.

12. Ciezak, J. A.; Byrd, E. F. C.; Rice, B. M. Exploring the High-Pressure Behavior of PETN: A Combined Quantum Mechanical and Experimental Study. Presented at the 25th Army Science Conference, Orlando, FL, November 2006.

13. Ciezak, J. A.; Trevino, S. F. Investigation of the Vibrational Spectroscopy of PETN by Inelastic Neutron Scattering and Solid State DFT Calculations. Unpublished work.

14. Dick, J. J. Effect of Crystal Orientation on Shock Initiation Sensitivity of Pentaerythritol Tetranitrate Explosive. *Appl. Phys. Lett*. **1984**, *44*, 859.

15. Dick, J. J.; Mulford, R. N.; Spencer, W. J.; Pettit, D. R.; Garcia, E.; Shaw, D. C. Shock Response of Pentaerythritol Tetranitrate Single Crystals. *J. Appl. Phys.* **1991**, *70*, 3572.

16. Dick, J. J. *Single Crystal Orientation Effects in Shock Initiation of PETN Explosive*; LA-UR-91-3413; Los Alamos National Laboratory: Los Alamos, NM, 1991.

17. Dick, J. J.; Ritchie, J. P. Molecular Mechanics Modeling of Shear and the Crystal Orientation Dependence of the Elastic Precursor Shock Strength in Pentaerythritol Tetranitrate. *J. Appl. Phys.* **1994**, *76*, 2726.

18. Dick, J. J. Anomalous Shock Initiation of Detonation in Pentaerythritol Tetranitrate Crystals. *J. Appl. Phys.* **1997**, *81*, 601.

19. Yoo, C. S.; Holmes, N. C.; Souers, P. C.; Wu, C. J.; Ree, F. H.; Dick, J. J. Anisotropic Shock Sensitivity and Detonation Temperature of Pentaerythritol Tetranitrate Single Crystal. *J. Appl. Phys.* **2000**, *88*, 70.

20. Dreger, Z. A.; Gruzdkov, Y. A.; Gupta, Y. M.; Dick, J. J. Shock Wave Induced Decomposition Chemistry of Pentaerythritol Tetranitrate Crystals: Time-Resolved Emission Spectroscopy. *J. Phys. Chem. B* **2002**, *106*, 247.

21. Hemmi, N.; Dreger, Z. A.; Gruzdkov, Y. A.; Winey, J. M.; Gupta, Y. M. Raman Spectra of Shock Compressed Pentaerythritol Tetranitrate Single Crystals: Anisotropic Response. *J. Phys. Chem. B* **2006**, *110*, 20,948.

22. Zaoui, A.; Sekkal, W. Molecular Dynamics Study of Mechanical and Thermodynamic Properties of Pentaerythritol Tetranitrate. *Solid State Commun*. **2001**, *118*, 345–350.

23. Gruzdkov, Y. A.; Dreger, Z. A.; Gupta, Y. M. Experimental and Theoretical Study of Pentaerythritol Tetranitrate Conformers. *J. Phys. Chem. A* **2004**, *108*, 6216.

24. Lipinska-Kalita, K. E.; Pravica, M. G.; Nicol, M. Raman Scattering Studies of the High-Pressure Stability of Pentaerythritol Tetranitrate, $C(CH_2ONO_2)_4$. *J. Phys. Chem. B* **2005**, *109*, 19,223.

25. Lipinska-Kalita, K. E.; Pravica, M. G.; Nicol, M. High-Pressure Synchrotron Radiation X-ray Diffraction Studies of Pentaerythritol Tetranitrate $C(CH_2ONO_2)_4$. In preparation.

26. Pravica, M.; Lipinkska-Kalita, K.; Quine, Z.; Romano, E.; Shen, Y.; Nicol, M. F.; Pravica, W. J. Studies of Phase Transitions in PETN at High Pressures. *J. Phys. Chem. Solids* **2006**, *67*, 2159.

27. Ciezak, J. A.; Jenkins, T. A. *New Outlook on the High-Pressure Behavior of Pentaerythritol Tetranitrate*; ARL-TR-4238; U.S. Army Research Laboratory: Aberdeen Proving Ground, MD, 2007.

28. Tschauner, O.; Kiefer, B.; Lee, Y.; Pravica, M.; Nicol, M.; Kim, E. Structural Transition of PETN-I to Ferroelastic Orthorhombic Phase PETN-III at Elevated Pressures. *J. Chem. Phys.* **2007**, *127*, 094502.

29. Dove, M. T. Theory of Displacive Phase Transitions in Minerals. *American Mineralogist* **1997**, *82*, 213.

30. Mao, H. K.; Xu, J.; Bell, P. M. Calibration of the Ruby Pressure Gauge to 800kbar Under Quasihydrostatic Conditions. *J. Geophys. Res.* **1986**, *91*, 4673.

31. Jayaraman, A. Diamond Anvil Cell and High-Pressure Physical Investigations. *Rev. Mod. Phys.* **1983**, *55*, 65.

32. Adar, F. Evolution and Revolution of Raman Instrumentation: Application of Available Technologies to Spectroscopy and Microscopy. In *Handbook of Raman Spectroscopy: From the Research Laboratory to the Process Line*; Lewis, I. R., Edwards, H. G. M., Eds.; Marcel Dekker, Inc.: New York, 2001; pp 11–41.

33. Liu, Z.; Yang, H.; Hu. J.; Mao, H. K.; Hemley, R. J. High Pressure Synchtrotron X-ray Diffraction and Infrared Microspectroscopy Applications of Dense Hydrous Phases. *J. Phys.: Condens. Matter* **2002**, *14*, 10,641.

34. Armstrong, R. W.; Elban, W. L. Dislocations in Energetic Crystals. In *Dislocations in Solids*; Nabarro, F. R. N., Hirth, J. P., Eds.; Elsevier, B. V.: Amsterdam, The Netherlands, 2004; Vol. 12, p 403.

NO. OF
COPIES ORGANIZATION

1 (PDF ONLY) DEFENSE TECHNICAL INFORMATION CTR
DTIC OCA
8725 JOHN J KINGMAN RD
STE 0944
FORT BELVOIR VA 22060-6218

1 US ARMY RSRCH DEV & ENGRG CMD
SYSTEMS OF SYSTEMS INTEGRATION
AMSRD SS T
6000 6TH ST STE 100
FORT BELVOIR VA 22060-5608

1 DIRECTOR
US ARMY RESEARCH LAB
IMNE ALC IMS
2800 POWDER MILL RD
ADELPHI MD 20783-1197

1 DIRECTOR
US ARMY RESEARCH LAB
AMSRD ARL CI OK TL
2800 POWDER MILL RD
ADELPHI MD 20783-1197

1 DIRECTOR
US ARMY RESEARCH LAB
AMSRD ARL CI OK T
2800 POWDER MILL RD
ADELPHI MD 20783-1197

ABERDEEN PROVING GROUND

1 DIR USARL
AMSRD ARL CI OK TP (BLDG 4600)

NO. OF COPIES ORGANIZATION

2 COMMANDER
US ARMY RSRCH OFC
TECH LIB
R ANTHENIAN
PO BOX 12211
RESEARCH TRIANGLE PARK NC
27709-2211

2 DIRECTOR
US ARMY RSRCH LAB
AMSRD ARL RO P
R SHAW
TECH LIB
PO BOX 12211
RESEARCH TRIANGLE PARK NC
27709-2211

4 COMMANDER
NAVAL RSRCH LAB
TECH LIB
CODE 4410
K KAILASANATE
J BORIS
E ORAN
4555 OVERLOOK AVE NW
WASHINGTON DC 20375-5000

1 OFFICE OF NAVAL RSRCH
CODE 473
J GOLDWASSER
800 N QUINCY ST
ARLINGTON VA 22217-5000

2 COMMANDER
NSWC
S MITCHELL
C GOTZMER
TECH LIB
INDIAN HEAD MD 20640-5000

1 COMMANDER
NAWC
INFO SCI DIV
CHINA LAKE CA 93555-6001

2 COMMANDER
NAWC
CODE 3895
CH1NA LAKE CA 93555-6001

NO. OF COPIES ORGANIZATION

1 WL MNME
ENERGETIC MTRL BR
2306 PERIMETER RD
STE 9
EGLIN AFB FL 32542-5910

1 DIRECTOR
SANDIA NATL LAB
M BAER
DEPT 1512
PO BOX 5800
ALBUQUERQUE NM 87185

2 DIRECTOR
LLNL
ALFRED BUCKINGHAM L 023
MILTON FINGER L 020
PO BOX 808
LIVERMORE CA 94550-0622

1 CIA
J BACKOFEN
RM 4PO7 NHB
WASHINGTON DC 20505

2 SRI INTRNTL
TECH LIB
PROPULSION SCI DIV
333 RAVENWOOD AVE
MENLO PARK CA 94025-3493

1 RDECOM ARDEC
TECH LIB
BLDG 59
PICATINNY ARSENAL NJ
07806-5000

1 AIR FORCE RSRCH LAB
MNME EN MAT BR
B WILSON
2306 PERIMETER RD
EGLIN AFB FL 32542-5910

1 AIR FORCE OFC OF SCI RSRCH
M BERMAN
875 N RANDOLPH ST
STE 235 RM 3112
ARLINGTON VA 22203-1768

NO. OF
COPIES ORGANIZATION

2 SANDIA NATL LABS
TECH LIB
NM BUILDING 804 MS-0899
ALBUQUERQUE NM 87185

2 LLNL
TECH/INFO DEPT LIB
PO BOX 808-L610
LIVERMORE CA 94550-0622

2 LOS ALAMOS NATL LAB
TECH LIB
MS-P362
PO BOX1663
LOS ALAMOS NM 87545-1362

3 NIST CENTER
FOR NEUTRON RESEARCH
T JENKINS
100 BUREAU DR MS8562
GAITHERSBURG MD 20899

ABERDEEN PROVING GROUND

16 DIR USARL
AMSRD ARL WM B
M ZOLTOSKI
AMSRD ARL WM BD
R BEYER
E BYRD
B FORCH
J CIEZAK (3 CPS)
K MCNESBY
M MCQUAID
R PESCE-RODRIGUEZ
B RICE
AMSRD ARL WM M
S MCKNIGHT
AMSRD ARL WM SG
T ROSENBERGER
AMSRD ARL WM T
B BURNS
P BAKER
AMSRD ARL WM TD
D DANDEKAR